Geomechanics and Engineering, *Vol. 14, No. 6 (2018) 509-517*
DOI: https://doi.org/10.12989/gae.2018.14.6.509

Modeling of pressuremeter tests to characterize the sands

Sadik Oztoprak[a], Sinan Sargin[b], Hidayet K. Uyar[c] and Ilknur Bozbey*

Faculty of Engineering, Department of Civil Engineering, Istanbul University, Avcilar 34320, Istanbul, Turkey

(Received July 28, 2017, Revised September 26, 2017, Accepted October 11, 2017)

Abstract. This paper proposes a numerical methodology for capturing the complete curve of a pressuremeter test including initial or disturbed parts and loops through a stiffness-based approach adopted in three dimensional finite difference code, FLAC3D. In order to enable this, a new hyperbolic model was used to replace the conventional linear elastic model prior to peak strength of Mohr-Coulomb soil model and update or degradation of shear modulus was considered. Presented modeling approach and implemented constitutive model are impressively successful. It leads to obtain the whole set of parameters for characterizing sands and seems promising for modeling the most of geotechnical structures.

Keywords: pressuremeter test; modified hyperbolic model; modulus evolution; small strain

1. Introduction

The measured pressure-volume (or displacement) responses of a pressuremeter test are related to the shear stiffness and strength properties of the soil. Advantage of this test is that it provides the deformation characteristics of soils. Although output of this test is the elastic modulus and the limit pressure in many countries, there are numerous works for modeling the stress-strain curve of the test. However, they are not that successful in capturing whole test procedures and the backbone curve. As seen in Fig. 1, test and soil type and drilling quality has an important effect on the stress-strain properties. Over-drilling or drilling in silty-sandy soil for pre-bored pressuremeter test may cause a delay for the response of soil (Fig. 1(a)). A disturbed part is inevitable and only after carrying out a loop, the soil may remediate. We can obtain minimum disturbed curves via pre-boring test in stiff clay or self-boring test in any soil (see Fig. 1(b)).

Decoding a test curve is of interest for many researchers. Hughes *et al.* (1977) developed a new interpretation of pressuremeter test in sand by using stress-dilatancy theory. Carter *et al.* (1986) proposed a closed form analytical solution for cavity expansion tests for both purely frictional and frictional cohesive material similar to Hughes *et al.* (1977). The procedure works in small strains and adopts the power law for describing the non-linear response for obtaining the parameters from unload/reload cycles. Manassero (1989) proposed a method for finding the friction angle ϕ and the dilatation angle ψ for sands.

Fahey and Carter (1993) expended a lot of effort attempting to simulate the expansion and contraction phases of a pressuremeter test but the authors achieved success only with unload-reload loops. However, they indicated that their main aim calibrating the modified hyperbolic model for use in the analysis of geotechnical structures was not compromised. For purely cohesive materials Whittle (1999) recommended a versatile curve matching procedure. On the other hand, Bolton and Whittle (1999) proposed a closed form solution for the undrained cavity expansion in a non-linear elastic perfectly plastic soil. The non-linear elastic response of soils with the characteristic that stiffness reduces with strain can be described by a power law. Geng *et al.* (2013) made an attempt to model pressuremeter test in sands through discreet element modelling. Although the authors found promising results, this modelling technique needs time for new achievements.

Yin and Hicher (2008), Frydman (2011), Likitlersuang *et al.* (2013), Savatier and Savatier (2016) and Balachandran *et al.* (2016) considered pressuremeter test results for determining, controlling and/or calibrating the soil parameters. A different approach was proposed by Emami and Yasrobi (2014) who enabled the numerical modelling of pressuremeter tests with the relations derived from artificial neural network. However, most researchers (Schanz *et al.* 1999, Monnet 2012, Sedran *et al.* 2013 and Fawaz *et al.* 2014) preferred to implement Mohr-Coulomb constitutive in axisymmetric condition for simulating the pressuremeter test. However, these works did not consider all the expansion and contraction phases of a pressuremeter test.

Oztoprak and Bolton (2011, 2013) indicated that the degradation of shear modulus causes non-linearity before plastic yielding, and this needs to be taken into account in deformation analyses for performance-based design of geotechnical structures. With this respect, Oztoprak and Bolton (2011) proposed a new hyperbolic model which was

*Corresponding author, Associate Professor
E-mail: ibozbey@istanbul.edu.tr
[a]Associate Professor
E-mail: oztoprak@istanbul.edu.tr
[b]Ph.D. Student
E-mail: ssargin@istanbul.edu.tr
[c]M.Sc. Student
E-mail: h.kemaluyar@hotmail.com

http://www.techno-press.org/?journal=gae&subpage=7 ISSN: 2005-307X (Print), 2092-6219 (Online)

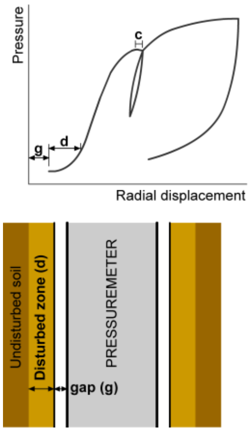

(a) Over-drilling or drilling in silty-sandy soil for pre-bored pressuremeter test

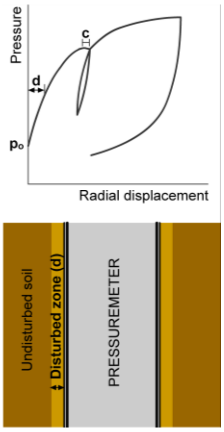

(b)Self-boring pressuremeter test in any soil or very good drilling in stiff clay for pre-bored pressuremeter

Fig. 1 Encountered installation effects and corresponding pressure-displacements curve

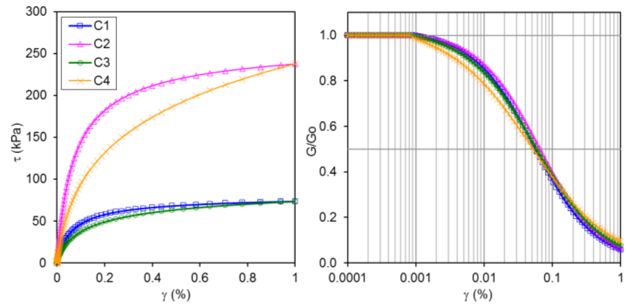

Curve	C1	C2	C3	C4
e	0.65	0.65	0.81	0.87
I_D	0.90	0.90	0.80	0.64
U_c	1.5	1.5	5.6	40.0
p' (kPa)	100	200	100	200
G_o (MPa)	128	363	97	250
γ_r (%)	0.056	0.065	0.058	0.051
γ_e (%)	9.E-04	1.E-03	9.E-04	8.E-04
a	0.97	0.97	0.88	0.76
$\phi_{1\%}$ (°)	36.1	58.3	36.1	58.3

Fig. 2 Evolution of shear stress-shear strain and normalized shear modulus-shear strain curves by using the modified hyperbolic model for different soils and stresses

used to replace the conventional linear elastic part prior to peak strength in the FLAC3D Strain Hardening/Softening Mohr Coulomb (SHS-MC) soil model. The performance of the model was checked by the pressuremeter test data in Thanet sands. It was demonstrated that a pressuremeter test in sand can be successfully modelled by considering the shear modulus reduction and by using combinations of soil parameters. Bahar and Belhassani (2012) presented that complete pressuremeter curve can be obtained through SHS-MC model in FLAC by considering the axisymmetric conditions.

In this paper, a modified version of Oztoprak and Bolton (2011) approach was proposed for analyzing a pressuremeter test in FLAC3D. This version incorporates the stress dependent shear modulus definition and compliance and disturbance of pressuremeter test for a complete and realistic modelling. By prescribed gap and creep amounts, a comprehensive modelling was provided.

2. Stiffness of sands and numerical modelling

Deformations of sandy soils around typical geotechnical structures display small to medium strain magnitudes under static loading. In this strain range, soils exhibit non-linear stress-strain behavior which should be incorporated in any deformation analysis. Oztoprak and Bolton (2013) developed modulus reduction curves by using a large amount of laboratory stiffness data for sandy soils which have been published since the 1970s and they refined the modified hyperbolic relationship of Darendeli (2001) to create a unique S-shaped curve of shear modulus reduction G/G_o given in Eq. (1)

$$\left(\frac{G}{G_o}\right) = \frac{1}{1+\left(\frac{\gamma-\gamma_e}{\gamma_r}\right)^a} \tag{1}$$

where γ_r, γ_e and a are as defined in Eqs. (2) to (4)

$$\gamma_r\,(\%) = 0.01 \cdot U_c^{-0.3} \cdot \left(\frac{p'}{p_a}\right) + 0.08 \cdot e \cdot I_D \tag{2}$$

$$\gamma_e\,(\%) = 0.0002 + 0.012 \cdot \gamma_r\,(\%) \tag{3}$$

$$a = U_c^{\;-0.075} \tag{4}$$

Three curve-fitting parameters were used: elastic threshold strain (γ_e), reference strain (γ_r) and curvature parameter (a). Reference strain is the post-elastic shear strain required to reduce G/G_o to 0.5 and this was found to depend on soil type (uniformity coefficient U_c), soil state (void ratio e and relative density I_D) and mean effective stress (p'). The elastic threshold strain was found to be linked to the reference strain, and the curvature parameter was found to be a function of the uniformity coefficient.

With the elastic stiffness data, Oztoprak and Bolton (2011) proposed a version of empirical relation by using void ratio (e), atmospheric pressure (p_a) and mean effective stress (p'). for the initial shear modulus, G_o

$$G_o = \frac{5760 \cdot p_a}{(1+e)^3} \cdot \left(\frac{p'}{p_a} \right)^{0.5} \tag{5}$$

Fig. 2 demonstrates the performance and sensitivity of developed stiffness model for 4 hypothetic sands. The model has the capability to evolve the G/G_o curves responsively when the U_c, e, I_D and p' change. For all curves, depending on the chosen parameters, stiffness model calculates varying friction angles assuming that plasticity does not evoke at strains lower than 1% in this case and that non-linear elasticity prevails regardless of the strain level. When the plasticity dominates the soil behavior in strain levels lower than 1%, these friction angles become lower.

2.1 Incorporating the new model in FLAC3D

FLAC3D is based on a continuum finite difference discretization using a Langrangian approach. Although this code has a number of built-in constitutive models for geomaterials, it also provides opportunity for modifying the current models or defining new ones through a macro programming language (FISH) which is embedded within FLAC3D.

In this paper, stiffness concept proposed by Oztoprak and Bolton (2013) was coupled with the strain-hardening/softening Mohr-Coulomb (SHS-MC) model to improve its performance in the small strain range. The SHS-MC model allows representation of nonlinear material softening and hardening behavior based on prescribed variations of the MC model properties (cohesion, friction, dilation, and tensile strength) as functions of the plastic shear strain which are not an output in the MC model. To incorporate the modified MC model in FLAC3D v5.0, FISH function was written for both versions, to represent the reduction of shear modulus during straining, up to failure. Stress dependent shear modulus calculations were carried out through another FISH function. Fig. 3(a) and 3(c) demonstrate the implemented stress-strain curve obtained by incorporating the modified hyperbolic relations for the pre-failure part and the perfectly plastic yield limit for the post-failure part of the stress-strain behavior in FLAC3D.

During a loading stage, corresponding shear modulus values (G) are obtained from the calculated modulus reduction curve through a FISH function using the stored shear strain increments ($ssi=\gamma$) which are always calculated from the starting point. In this respect, to incorporate the modified hyperbolic model in FLAC3D, a FISH function was written to represent the reduction of shear modulus during straining. Fig. 3(a) shows how the proposed model handles the evolution of stress-strain curve by using the shear modulus degradation defined in Fig. 3(b). Eventually, achieved stress-strain curve can be seen in Fig. 3(c).

The MC (also the SHS-MC) model is used for materials that yield when subjected to shear loading; a shear yield function and a non-associated shear flow rule are used. In addition, the failure envelope for the model is characterized by a tensile yield function with associated flow rule. The yield stress (f_s) depends on the major and minor principal stresses (σ_1 and σ_3 respectively) only; the intermediate principal stress (σ_2) has no effect on yield. In the original MC model (also the SHS-MC model), the stress-strain curve is linear up to the point of yield (Fig. 3(a) and 3(c)); in that range, the strain is elastic only: $\gamma = \gamma^e$. After yield, the total strain is composed of elastic and plastic parts: $\gamma = \gamma^e + \gamma^p$. The stress to cause shear failure in the FLAC3D MC model is defined as

$$f^S = \sigma_1 - \sigma_3 N_\phi + 2c\sqrt{N_\phi} \tag{6}$$

where

$$N_\phi = (1 - \sin\phi)/(1 + \sin\phi) \tag{7}$$

Here; c is cohesion, and ϕ is friction angle. Beyond peak strength, soil plasticity was invoked, using Rowe's stress-dilatancy with constant friction angle (ϕ) and dilation angle (ψ). The plastic potential is given by

$$g^S = \sigma_1 - \sigma_3 N_\psi \tag{8}$$

where

$$N_\psi = (1 - \sin\psi)/(1 + \sin\psi) \tag{9}$$

The developed model can be defined as a modified hyperbolic model using MC yield surface. The procedure of the adopted model is given below:

i. Initial reference shear modulus values (G_o^{ref}) of each element are defined by Eq. (10). Afterwards, G_o values are assigned through Eq. (11).

$$G_o^{ref} = f \cdot \frac{5760 \cdot p^{ref}}{(1+e)^3} \cdot \left(\frac{p'}{p^{ref}} \right)^{0.5} \tag{10}$$

$$G_o = G_o^{ref} \cdot \left(\frac{c \cdot \cos\phi - p' \cdot \sin\phi}{c \cdot \cos\phi + p^{ref} \cdot \sin\phi} \right)^m \tag{11}$$

Here, p_{ref} is the mean effective stress $[(\sigma_x+\sigma_y+\sigma_z)/3]$ at the test depth, p' is the corresponding mean effective stress at the achieved loading state and m is stiffness exponent. According to Janbu (1963), PLAXIS (2014) and FLAC3D (2016) it is between 0 and 1.

ii. Calculated incremental shear strain (ssi) values are stored after the calculations for each zone.

iii. Corresponding shear modulus values are obtained from the calculated modulus reduction curve given in Eqs. (1)-(4) through a FISH function using the stored ssi values. The function always uses the elastic part (γ_e) of the ssi as the value of γ to be used in Eq. (3). It means that $ssi=\gamma_e$ before yielding and $ssi=\gamma_e+\gamma_p$ afterwards

iv. Grid point displacements are updated with the new incremental strains. The program proceeds to the next loading stage. The developed model can be defined as non-linear elastic perfectly plastic model in which a modified hyperbola controls the stiffness behavior and MC yield surface controls the plasticity. The procedure of the adopted models demonstrated in Fig. 3.

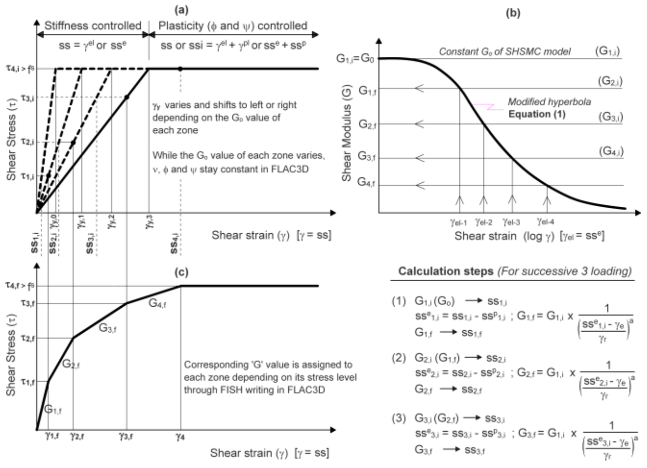

Fig. 3 Adopted procedure of non-linear elastic perfectly plastic model in FLAC3D

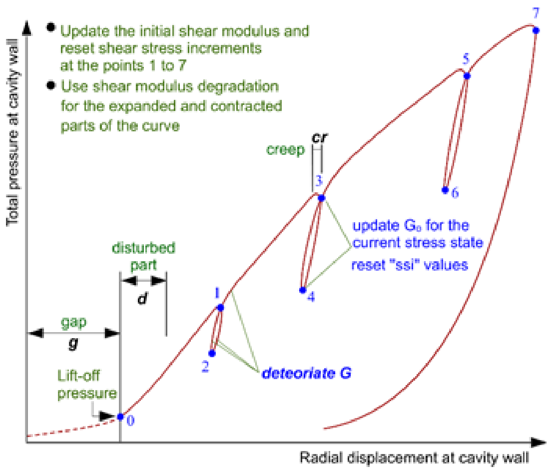

(a) Presentation of modelling steps in FLAC3D

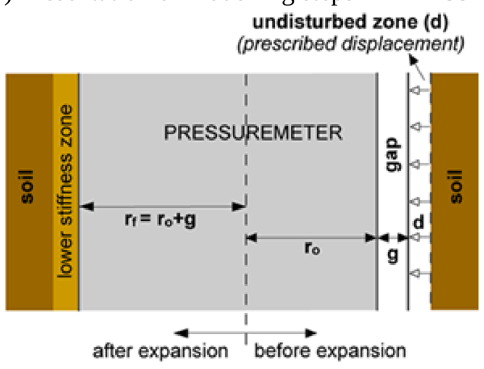

(b) Definition of parameters

Fig. 4 Modelling of pressuremeter test

2.2 Pressuremeter Modelling in FLAC3D and Applications

The measured pressure-volume (or radius) response of a pressuremeter test is related to the shear stiffness and strength properties of soil. However, varying stress and strain conditions around the instrument are complicated. Therefore, this causes difficulties in simulating the whole stress-strain behavior including unload-reload loops.

This paper, similar to Fahey and Carter (1993), proposes a hyperbolic model with Mohr-Coulomb yield surface to model a pressuremeter test. Proposed hyperbolic model, however, considers the soil type, soil state and mean effective stress. Since the developed stiffness degradation equations are adequate for numerical modelling, the model was readily incorporated in FLAC3D software.

For numerical modeling of a pressuremeter test, evolution of G and G_o should be defined. As demonstrated in Fig. 4(a), initial shear modulus (G_o) values are automatically updated through the equations (10) and (11) at points 1 to 7 according to each zone's mean effective stresses. Updating G_o only at reversal of loading is similar to the approach applied by Fahey and Carter (1993). It was also needed to reset the shear strain increment (*ssi*) values of the zones every time after changing the direction of load. In addition to this, secant shear modulus were allowed to be degraded during loading and unloading by using the Eqs. (1)-(4). All these calculations are carried out by using two FISH functions.

The initial part of the curve of a pressuremeter test may be affected by the compliance of the instrument to the cavity (g) and disturbance due to drilling (d). This effect was tried to be modelled in this paper. The gap (g) between the membrane and cavity wall and the thickness of the disturbed soil zone (d) were included in the procedure to capture the initial curve (Fig. 4(b)). According to the soil and pressuremeter type, g and d may be larger and therefore should be included in the numerical modeling. Execution of loops during a pressuremeter test is important to recover the disturbed initial part of test curve. On the other hand, for stiffness-based modeling of a pressuremeter test, number of loops has crucial importance, since the location, inclination, and size of loops are affected by the stiffness parameters. Just before starting a loop or final unloading, creep stage is required for establishing static equilibrium and stiffness prevalence. However, modelling of creep stage is out of scope of this study. Therefore, creep displacements (*cr* in Fig. 4(a)) were determined from a test curve and manually added into the obtained pressure-displacement curve from numerical analyses.

To apply the model and verify its success, three self-boring pressuremeter tests each including three loops were selected. Test curves, their depth and lift-off pressures can be seen in Fig. 5. The tests were performed by Cambridge Insitu Ltd and were carried out in the Thanet sand at Woolwich. Thanet sand is generally described as over-consolidated, very dense, grey, silty, quarzitic, and fine sand which lies beneath the London clay in central London (Ventouras, 2005). According to Arup Geotechnics (2000), Thanet sand has an over consolidation ratio changing from 4 to 8 which causes high values of K_o.

The lateral earth pressure coefficient K_o, which is an important input parameter for any numerical analysis, is estimated by using 'lift-off' pressure ($p_{h,o}$). For the initial attempts for estimating ϕ, the method of Hughes *et al.* (1977), Carter *et al.* (1986) or Manassero (1989) can be used. The constant volume friction angle was selected as around ϕ_{cv}=33° and $\phi_p=\phi_{cv}+0.8\psi$ equation of Bolton (1986) was used to find ψ values.

After fixing earth pressure coefficient at-rest (K_o),

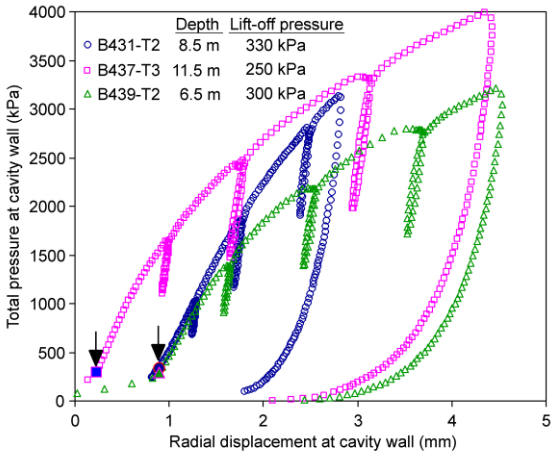

Fig. 5 Field curves of SBP tests carried out by Cambridge Insitu Ltd at Woolwich (Oztoprak and Bolton 2011)

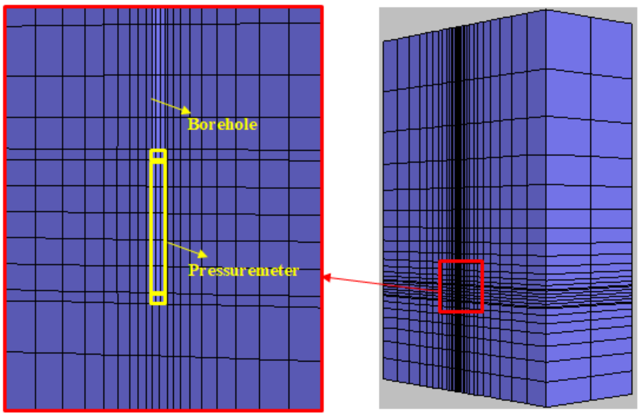

Fig. 6 Constructed 3D model and defined finite element mesh for test B31-T2 in FLAC3D

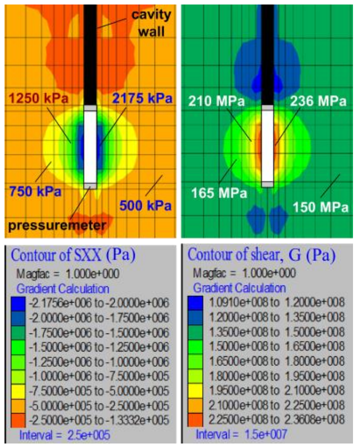

(a) At full expansion phase

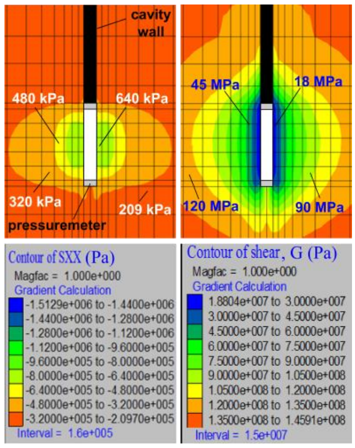

(b) At full contraction phase

Fig. 7 Variation of horizontal stress and shear modulus around pressuremeter for test B31-T2

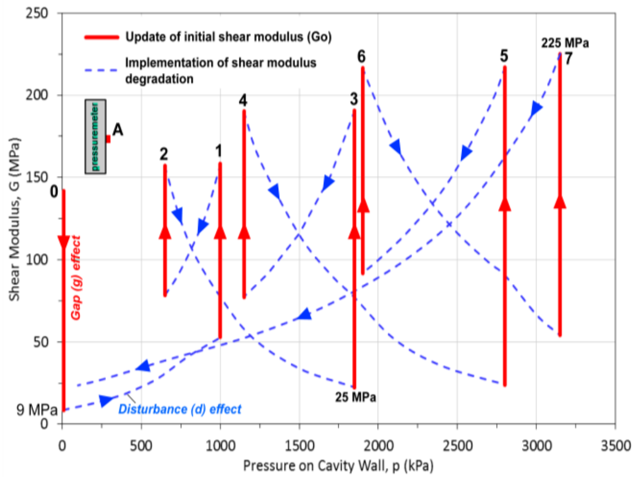

Fig. 8 Variation of shear modulus at the closest zone (zone A) to the pressuremeter during the test of B31-T2 (numbers next to thick vertical lines correspond to numbers in Fig. 4)

Poisson's ratio (v), shear strength angle (ϕ) and dilatancy angle (ψ) with the above approaches, reading gap (g) and creep (cr) values from the curve and adjusting the inclination and size of the loops, gap (g), disturbance (d), shear modulus adjusting factor (f) and shear modulus power coefficient (m) are investigated for capturing the location of loops and whole curve. Constructed 3D model and corresponding meshing around pressuremeter test can be seen in Fig. 6.

3. Results

In order to demonstrate the horizontal effective stress and shear modulus contours, two different load cases were selected. Fig. 7(a) depicts the full expansion phase contours for horizontal stress and shear modulus and Fig. 7(b) demonstrates the full contraction phase contours for horizontal stress and shear modulus. Contours of shear modulus for both expansion and contraction phases reveal the success of the proposed approach in modelling the evolution of shear modulus. Fig. 8 briefly shows how the proposed approach modifies the shear modulus approximately all over the test. Starting with the G_o=142 MPa for zone 'A', it goes up G=225 MPa after the creeps before the loops and drops down to G=25 MPa at the unloading parts of loops. Figs. 9-11 show the field and simulated curves of three selected SBP tests; B439-T2, B431-T2, and B437-T3 respectively.

The curves given by the best fit parameters were compared with the field data of B439-T2 test. In relation to

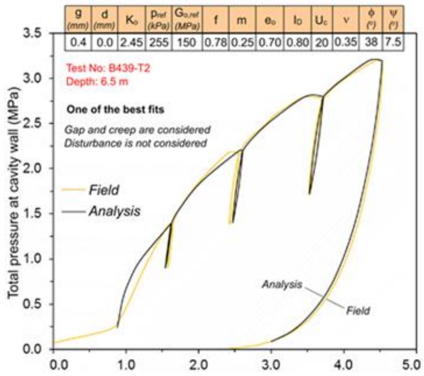

(a)

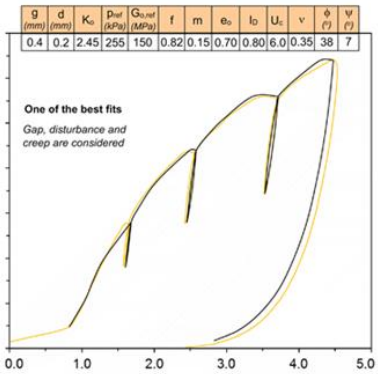

(b)

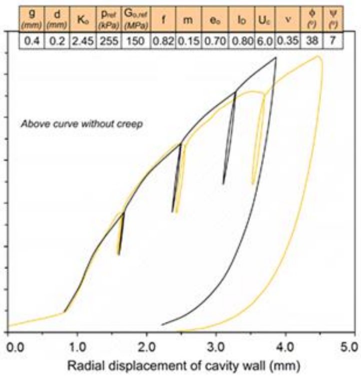

(c)

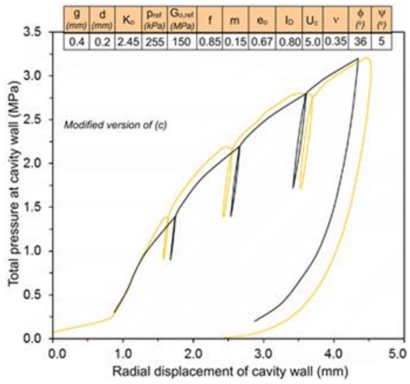

(d)

Fig. 9 Obtained curves from the analyses of B439-T2 test

this, Fig. 9(a) and 9(b) discuss the effect of disturbance. If the disturbance of the sand around pressuremeter was not taken into account, the first expansion phase of the curve was not that successful, however, last expansion and

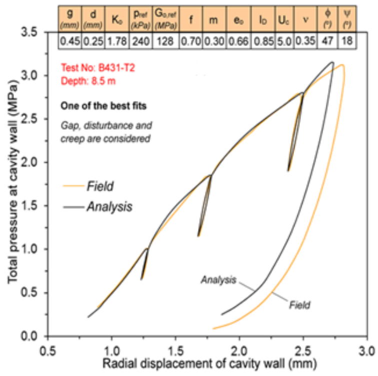

(a)

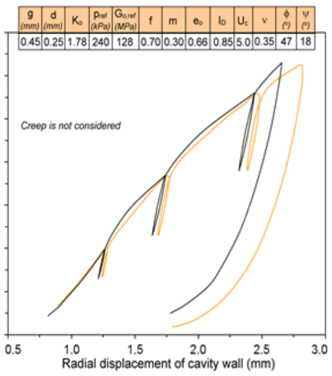

(b)

Fig. 10 Obtained curves from the analyses of B431-T2 test

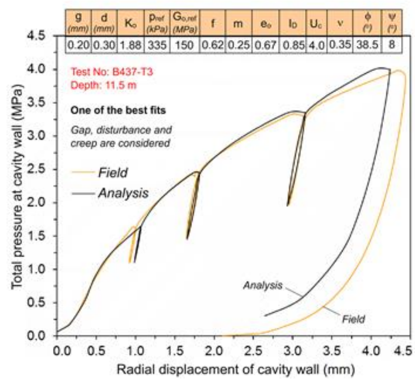

(a)

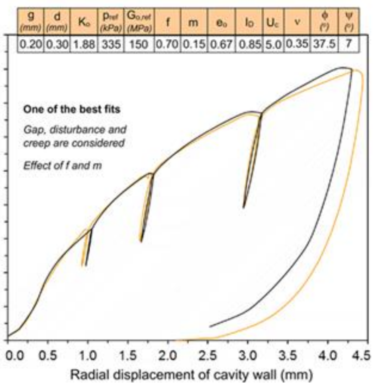

(b)

Fig. 11 Obtained curves from the analyses of B437-T3 test

unloading curves were perfectly captured. Fig. 9(b) and 9(c) discusses the effect of creep (*cr*). After making proper adjustment on the parameters of Figs. 9(c) and 9(d) can be obtained. As seen from Fig. 9(d), test curve was less affected by the creep amount (approximately 2° both for ϕ and ψ).

Best fit curves of B431-T2 and B437-T3 tests depicted in Figs. 10-11. These figures demonstrate how the analyses are successful for fitting the field curves. Fig. 10(b) shows an example that it is possible to obtain similar parameters without defining creep. Fig. 11(b) also shows that different *f* and *m* values has effect on the strength parameters.

As discussed above, results exhibited that the developed approach is very successful in capturing complete curve of any pressuremeter test. In particular, the modified hyperbolic model has proved its ability in quite accurately reproducing the size and inclination of the loops. Following results were achieved about the effects and interchangeability of parameters on the pressure-displacement curves:

a. Earth pressure coefficient at-rest (K_o) affected the whole curve, including the sizes of the loops, but not their inclination. This important parameter can successfully be estimated from the lift-off pressure.

b. The gap (*g*) between instrument and the cavity and the thickness of the disturbed zone (*d*) enabled a nice touch on the initial part of the curve. It was also prevented the shifting of axis. Disturbance (*d*) made a corresponding reduction on shear modulus at the zones close to the pressuremeter. After starting the first expansion, each zone commenced its movement from the current position on the G/G_o-γ curve. It was seen that *g* and *d* are not independent from the other parameters.

c. Locations of the loops are very important in understanding the parameter effect. With and without supplemental creep amount, parameters, especially shear strength angle (ϕ) and dilatancy angle (ψ), were slightly changed.

d. Reference initial shear modulus ($G_{o,ref}$) and mean stress at the middle of the pressuremeter probe (p_{ref}) adjust the evolution of initial shear modulus by stress. Shear modulus adjusting factor (*f*) and shear modulus power coefficient (*m*) values are quite helpful for finding the appropriate G_o.

e. Void ratio (*e*) and Poisson's ratio (*v*) were kept constant during the analyses. Although the *v* is related to the stress, it was fixed to 0.35. Poisson's ratio was compensated with ϕ and ψ. In case it was decreased, ϕ and ψ needed to be increased. The reverse was also valid. K_o and *v* also present similar behavior.

4. Conclusions

A new approach was proposed for numerical modeling of the pressuremeter test. It was demonstrated that a pressuremeter test can successfully be modelled through the proposed hyperbolic model and adopted procedure which considers stiffness evolution in finite difference code, FLAC3D. In this context, proposed numerical model is versatile to verify the parameters of initial shear modulus equation. To enable this, the gap between the instrument and cavity wall and the thickness of disturbed zone are also considered. In addition to this, shear modulus of the zones around the pressuremeter are updated continuously depending on the mean effective stress, void ratio, relative density and uniformity coefficient during expansion and contraction phases. Lateral earth pressure coefficient was found to have crucial importance on the overall behavior including stiffness and shear strength parameters. Other conclusions can be drawn as below:

- To model the small strain behavior and therefore to obtain the corresponding shear modulus and index properties of the tested soils, the loops are of crucial importance.
- The size, and inclination of the loops are completely related with the degradation behavior of shear modulus.
- At least two loops are necessary to implement the proposed approach. More loops lead to better soil characterization.
- Initial part of a pressuremeter curve was successfully modeled by defining the gap between instrument and the cavity, and estimating the thickness of the disturbed zone.
- Locations of the loops provided valuable help during the back-analyses of a test curve. It was seen that supplemental creep amount affects the parameters slightly.
- Implementation of the procedure needs thirteen parameters. Most of them can easily be deduced from the curve and basic laboratory and field tests.
- Different parameter combinations are valid for a soil and pressuremeter test provides a unique and versatile way to obtain these parameters.
- Implementing the deduced parameter combination from a pressuremeter test would lead to realistic results in numerical modeling of a geotechnical problem. Otherwise, collecting different parameters from different tests may lead to erroneous results.

Acknowledgements

This work was supported by Scientific Research Projects Coordination Unit of Istanbul University, Project No: BYP-35683. The authors would like to thank Robert Whittle and Cambridge Insitu Ltd. for supplying the pressuremeter data. The first author indebted to Prof. Malcolm Bolton who initiated this research during his visit to Cambridge University.

References

Arup Geotechnics (2000), *Building HQ1, Factual Geotechnical Information Package*.

Bahar, R. and Belhassani, O. (2012), "Numerical analysis of a cyclic pressuremeter test", *Proceedings of the 15th World Conference on Earthquake Engineering*, Lisbon, Portugal, September.

Balachandran, K., Liu, J., Cao, L. and Peaker, S. (2016), "Finite element simulation of pressuremeter test in glacial tills", *Proceedings of the 69th Canadian Geotechnical Conference, GeoVancouver 2016*, Vancouver, Canada, October.

Bolton, M.D. (1986), "The strength and dilatancy of sands", *Géotechnique*, **36**(1), 65-78.

Bolton, M.D. and Whittle, R.W. (1999), "A non-linear

elastic/perfectly plastic analysis for plane strain undrained expansion tests", *Géotechnique*, **49**(1), 133-141.
Cambridge Insitu Ltd., <http://www.cambridge-insitu.com>.
Carter, I.P., Booker, J.R. and Yeung, S.K. (1986), "Cavity expansion in cohesive frictional soils", *Géotechnique*, **36**(3), 349-358.
Darendeli, B.M. (2001), "Developement of a new family of normalize modulus reduction and material damping curves", Ph.D. Dissertation, University of Texas at Austin, Austin, Texas, U.S.A.
Emami, M. and Yasrobi, S.S. (2014), "Modeling and interpretation of pressuremeter test results with artificial neural networks", *Geotech. Geol. Eng.*, **32**(2), 375-389.
Fahey, M. and Carter, J.P. (1993), "A finite element study of the pressuremeter test in sand using a nonlinear elastic plastic model", *Can. Geotech. J.*, **30**(2), 348-362.
Fawaz, A., Hagechehade, F. and Farah, E. (2014), "A study of the pressuremeter modulus and its comparison to the elastic modulus of soil", *Stud. Civ. Eng. Arch.*, **3**, 7-15.
FLAC3D (2016), *Fast Langrangian Analysis of Continua-Manual*, Itasca Consulting Group, Minnesota, USA.
Frydman, S. (2011), "Characterizing the geotechnical properties of natural Israeli, partially cemented sands", *Geomech. Eng.*, **2**(4), 323-337.
Geng, Y., Yu, H.S. and McDowell, G.R. (2013), "Discrete element modelling of cavity expansion and pressuremeter test, *Geomech. Geoeng.*, **8**(3), 179-190.
Hughes, J.M.O, Wroth, C.P. and Windle, D. (1977), "Pressuremeter tests in sands", *Géotechnique*, **27**(4), 455-477.
Janbu, N. (1963), "Soil compressibility as determined by oedometer and triaxial tests", *Proceedings of the 3rd European Conference on Soil Mechanics and Foundation Engineering*, Weisbachen, Germany, October.
Likitlersuang, S., Surarak, C., Wanatowski, D., Oh, E. and Balasubramaniam, A. (2013), "Geotechnical parameters from pressuremeter tests for MRT blue line extension in Bangkok", *Geomech. Geoeng.*, **5**(2), 99-118.
Manassero M. (1989), "Stress strain relationships from drained self-boring pressuremeter tests in sands", *Géotechnique*, **39**(2), 293-307.
Monnet, J. (2012), "Elasto-plastic analysis of the pressuremeter test in granular soil part 2: Numerical study", *Eur. J. Environ. Civ. Eng.*, **16**(6), 715-729.
Oztoprak, S. and Bolton, M.D. (2011), "Parameter calibration of a modified hyperbolic model for sands using pressuremeter test data", *Proceedings of* 5*th International Symposium on Deformation Characteristics of Geomaterials*, Seoul, Korea, September.
Oztoprak, S. and Bolton, M.D. (2013), "Stiffness of sands through a laboratory test database", *Géotechnique*, **63**(1), 54-70.
PLAXIS (2014), *Material Models Manual*.
Savatier, V. and Savatier, M. (2016), "Stress path during pressuremeter test and link between shear modulus and menard pressuremeter modulus in unsaturated fine soils", *Proceedings of the 3rd European Conference on Unsaturated Soils*, Paris, France, September.
Schanz, T., Vermeer, P.A. and Bonnier, P.G. (1999), *The Hardening Soil Model: Formulation and Verification*, in *Beyond 2000 in Computational Geotechnics*, A.A. Balkema, Rotterdam, The Netherlands.
Sedran, G., Failmezger, R.A. and Drevininkas, A. (2013), "Relationship between menard (EM) and Young's (E) moduli for cohesionless soils", *Proceedings of the 18th International Conference on Soil Mechanics and Geotechnical Engineering*, Paris, France, September.
Ventouras, K. (2005), "Engineering properties of Thanet sand", Ph.D. Dissertation, Imperial College of Science, Technology and Medicine, London, U.K.
Whittle, R.W. (1999), "Using non-linear elasticity to obtain the engineering properties of clay-a new solution for the self-boring pressuremeter", *Ground Eng.*, **32**(5), 30-34
Yin, Z. and Hicher, P.Y. (2008), "Identifying parameters controlling soil delayed behaviour from laboratory and in situ pressuremeter testing", *J. Numer. Anal. Meth. Geomech.*, **32**(12), 1515-1535.

CC

Appendix

a Curvature parameter

c Cohesion

cr Creep

d Thickness of the disturbed zone due to drilling

f Soil type factor for shear modulus

f^S Mohr-Coulomb yield function in Flac3D

f_s Yield stress

e Void ratio

g Width of gap between pressuremeter and cavity wall

g^S Shear potential function of MC model in Flac3D

G_o Initial shear modulus

G Shear modulus at any strain level

G/G_o Normalized shear modulus

G_o^{ref} Initial reference shear modulus

I_D Relative density

K_o Lateral earth pressure at rest

m Stiffness exponent

$N\phi$ Flow value for yield function

N_ψ Flow value for shear potential

p' Mean effective stress

p_a Atmospheric pressure

$p_{h,o}$ Lift-off pressure

p_{ref} Reference stress

r_f Final diameter of cavity hole

r_o Initial diameter of cavity hole

ssi Incremental shear strain

U_c Uniformity coefficient

ϕ friction angle

ϕ_p Peak friction angle

ϕ_{cv} Constant volume friction angle

γ_e Elastic threshold strain

γ_r Reference strain

γ Shear strain

γ^e Elastic shear strain

γ^p Plastic shear strain

γ_y Yield shear strain

ψ dilatation angle

v Poisson's ratio

σ_x Lateral stress in x direction

σ_y Lateral stress in y direction

σ_z Vertical stress

σ_1 Major principal stress

σ_2 Intermediate principal stress

σ_3 Minor principal stress

τ Shear stress